FRIGID ZONE **MEDICINE**
Original Article • DOI: 10.1515/fzm-2025-0024

Comprehensive analysis of cold exposure-associated transcriptional and metabolic changes in the liver

Yuzhu Di[1#], Zhengchao Wen[2#], Xiaomin Liu[2], Kejiao Zhang[2], Xiuyun Shen[2,3], Chunpeng Shi[2], Yuqiu Chao[2,3,4], Xiao Wang[2], Shu Wang[5], Bo Qu[1*], Yanan Jiang[2,3,4*]

Abstract

Background: Cold exposure is associated with metabolic alterations. This study aims to investigate the effects and mechanisms of cold exposure on liver metabolism through the integration of transcriptomics and metabolomics. **Methods:** Liver tissues from mice exposed to cold were subjected to RNA sequencing and liquid chromatography-mass spectrometry (LC-MS) for transcriptomic and metabolomic profiling, respectively. Differentially expressed genes (DEGs) and differentially expressed metabolites (DEMs) were identified. mRNA expression levels were validated by real-time polymerase chain reaction (RT-PCR). Gene ontology (GO), Kyoto encyclopedia of genes and genomes (KEGG), and Reactome enrichment analyses were performed. Finally, transcriptomic and metabolomic data were integrated and analyzed. **Results:** Cold exposure altered the transcriptomic and metabolomic profiles in the liver in cold exposed mice. Enrichment analyses were of DEGs and DEMs. Enrichment analyses of DEGs and DEMs revealed that DEGs were involved in pathways such as the PI3K-Akt signaling pathway, cytokine-cytokine receptor interaction, and cell adhesion molecules. DEMs were enriched in pathways related to membrane transport, nucleotide metabolism, and the metabolism of cofactors and vitamins. The integration of transcriptomic and metabolomic data identified several pathways potentially associated with cold exposure, such as the PI3K-Akt signaling pathway. **Conclusion:** Cold exposure alters liver transcriptomic and metabolomic profiles in mice. The integrative analysis of transcriptomic and metabolomic data highlights the complexity of the liver's response to cold exposure and identifies potential targets for further investigation.

Keywords

cold exposure; liver metabolism; transcriptome; metabolome

Received 06 March 2024, accepted 23 February 2025

[1]*Department of Gastroenterology and Hepatology, the Second Affiliated Hospital of Harbin Medical University, Harbin 150081, China*
[2]*Department of Pharmacology (National Key Laboratory of Frigid Zone Cardiovascular Diseases, the State-Province Key Laboratories of Biomedicine-Pharmaceutics of China, Key Laboratory of Cardiovascular Research, Ministry of Education), College of Pharmacy, Harbin Medical University, Harbin 150081, China*
[3]*Translational Medicine Research and Cooperation Center of Northern China, Heilongjiang Academy of Medical Sciences, Harbin 150081, China*
[4]*Department of Oral and Maxillofacial Surgery, the First Affiliated Hospital, Harbin Medical University, Harbin 150081, China*
[5]*Department of Cardiology, the First Affiliated Hospital of Harbin Medical University, Harbin 150081, China*

**Corresponding authors Yanan Jiang, E-mail: jiangyanan@hrbmu.edu.cn; Bo Qu, E-mail: qubo_1970@hotmail.com*
[#]*These authors contributed equally to this work.*

1 Introduction

The climate or environmental temperature can significantly affect human physiological status[1].This is particularly concerning for the health of individuals living in high-latitude regions, where winters are long and temperatures can be extremely low.

Epidemiological studies have shown that people residing in cold regions are more susceptible to certain diseases, such as cardiovascular diseases and liver diseases[2-3]. A cross-sectional study identified cold seasons as an independent risk factor for metabolic-dysfunction-associated fatty liver disease (MAFLD)[3]. Additionally, another study reported that the prevalence of MAFLD in northern China is 19% higher than that in southern China[4], a phenomenon potentially associated with cold climate conditions and regional lifestyle habits.

Furthermore, exposure to a cold environment can trigger a harmful inflammatory response in the liver, potentially contributing to hepatitis and other liver-related diseases. In a study involving mice subjected to chronic cold stress, Liu *et al.* confirmed that cold exposure induced liver cell apoptosis and pyroptosis, while promoting the release of pro-inflammatory cytokines[5]. Conversely, cold exposure has also been reported to have beneficial effects on certain conditions. For example, a study found that cold exposure improved insulin sensitivity in patients with type 2 diabetes[6], and

appropriate cold stimulation has been shown to alleviate muscle soreness after exercise[7].

Cold exposure induces metabolic reprogramming, particularly affecting the liver function. In response to cold stimulation, the liver produces heat and releases glucose to maintain euglycemia and core body temperature. Several preclinical studies have reported a significant reduction in hepatic glycogen content in cold-exposed rats[8-9]. Xu *et al.* found that cold exposure upregulated the expression of gluconeogenic genes in the liver, thereby enhancing hepatic gluconeogenesis in male mice[10]. In addition, untargeted metabolomics has been employed to investigate the metabolic changes induced by cold exposure in mice[11]. Certain genes, such as uncoupling proteins 4 (UCP4) and UCP5, have been found to be susceptible to dietary and temperature manipulations[12]. However, a comprehensive analysis of liver transcriptional and metabolic changes in response to cold exposure remains lacking.

In this study, we comprehensively analyze cold exposure-induced liver transcriptional and metabolic abnormalities in the liver by integrating transcriptomic and metabolomic data.

2 Materials and methods

2.1 Animal model establishment and treatment

C57BL/6 mice (20-22g) were purchased from Liaoning Changsheng Biotechnology Co., Ltd. (Liaoning, China). All mice were randomly assigned to the control, day, and night groups. With the same strain, age, and gender, the mice were maintained on a standardized diet throughout the study. Mice in the control group were housed at room temperature. In the day group, mice were exposed to 12 h of light at 4°C, followed by 12 h of darkness at room temperature. In contrast, mice in the night group were subjected to the opposite conditions, experiencing 12 h of darkness at 4°C and 12 h of light at room temperature. After one month of treatment, physiological indicators were assessed, and samples were collected. All experimental procedures were approved by the Laboratory Animal Ethics Committee of Harbin Medical University (IRB3057723).

2.2 RT-PCR analysis

Total RNA was extracted using TRIzol reagent (Takara, Japan). The RNA was then reverse transcribed into cDNA using ReverTra Ace qPCR RT kit (Toyobo, Japan). The RNA was then reverse-transcribed into cDNA using the ReverTra Ace qPCR RT kit (Toyobo, Japan). Quantitative PCR (qPCR) was performed on an ABI 7500 Fast RT-PCR System (Applied Biosystems, USA) using SYBR Green I (Toyobo, Japan). Relative gene expression levels were calculated using the $2^{-\Delta\Delta CT}$ method.

The primer sequences used were as follows: Arntl forward 5'-CCAGGGTTTGAAGTTAGAGTCC-3', reverse 5'-TGAAGTCGCTGATGGTTGAG-3', Cry1 forward 5'-AGGAGGACAGATCCCAATGGA, reverse AGGAGGACAGATCCCAATGGA; Col1a1 forward 5'-TCCGGCTCCTGCTCCTCTTA, reverse TCCGGCTCCTGCTCCTCTTA; Egf forward 5'-TACTCAGCGTCACAGCATGG, reverse TACTCAGCGTCACAGCATGG; GAPDH forward 5'-AAGAAGGTGGTGAAGCAGGC, reverse TCCACCACCCTGTTGCTGTA.

2.3 Transcriptome analysis

RNA sequencing was performed on the Illumina Novaseq 6000 platform by Shanghai OE Biotech Co., Ltd. Sequencing results were aligned to the reference genome using Hisat2 software[13]. Differentially expressed genes (DEGs) were identified based on a $\log_2$ fold change (FC) > 1 and $P < 0.05$. Hierarchical clustering analysis of DEGs was performed using R (V3.2.0) to visualize gene expression patterns across different groups and samples.

2.4 Metabolomics analysis

Raw liquid chromatography-mass spectrometry (LC-MS) data were processed using Progenesis QI v2.3 software (Nonlinear Dynamics, Newcastle, UK), including baseline filtering, peak identification, integration, retention time correction, peak alignment, and normalization. Metabolites were extracted from mouse liver tissue[14]. The processed data matrix was imported into R for orthogonal partial least squares-discriminant analysis (OPLS-DA) to distinguish differential metabolites between groups. The overall contribution of each variable to group discrimination was ranked based on variable importance in projection (VIP) values obtained from the OPLS-DA model. A two-tailed *t*-test was performed to determine the statistical significance of between-group differential metabolites. Metabolites with VIP > 1.0 and $P < 0.05$ were considered significant.

2.5 Enrichment analysis

Gene ontology (GO)[15] and kyoto encyclopedia of genes and genomes (KEGG)[16] pathway enrichment analyses were performed on DEGs using a hypergeometric distribution approach. Significantly enriched terms were identified using R (v3.2.0). Graphs were also generated using R (v3.2.0).

2.6 Gene set enrichment analysis

Gene set enrichment analysis (GSEA) was performed using the GSEA software[17]. This analysis uses predefined gene sets and ranks genes based on their degree of differential expression between the two sample groups. The predefined gene sets were then assessed to determine whether they were significantly

enriched at the top or bottom of the ranked gene list.

2.7 The integration of transcriptomics and metabolomics

Transcriptomic and metabolomic data were considered correlated if they accumulated in the same sample. DEG- differentially expressed metabolite (DEM) - pairs with Pearson correlation coefficients of $P < 0.05$ were selected for further analysis. Correlation plots were generated for comparative analysis, followed by KEGG pathway enrichment analysis. KEGG pathway enrichment analysis was then performed. Additionally, homologous DEGs and DEMs were mapped to reference pathways in the KEGG database to better understand their regulatory roles within these pathways.

2.8 Statistical analysis

All experimental results are expressed as mean ± standard error of the mean (SEM). Comparisons between groups were performed using a *t*-test. A two-tailed $P < 0.05$ was considered statistically significant.

3 Results

3.1 Identification of DEGs in the liver of cold-exposed mice

The mRNA expression profiles of liver tissues were analyzed using RNA sequencing. Hierarchical cluster analysis revealed distinct gene expression patterns across the different groups (Fig. 1A and B). DEGs were identified based on a $\log_2$ FC > 1

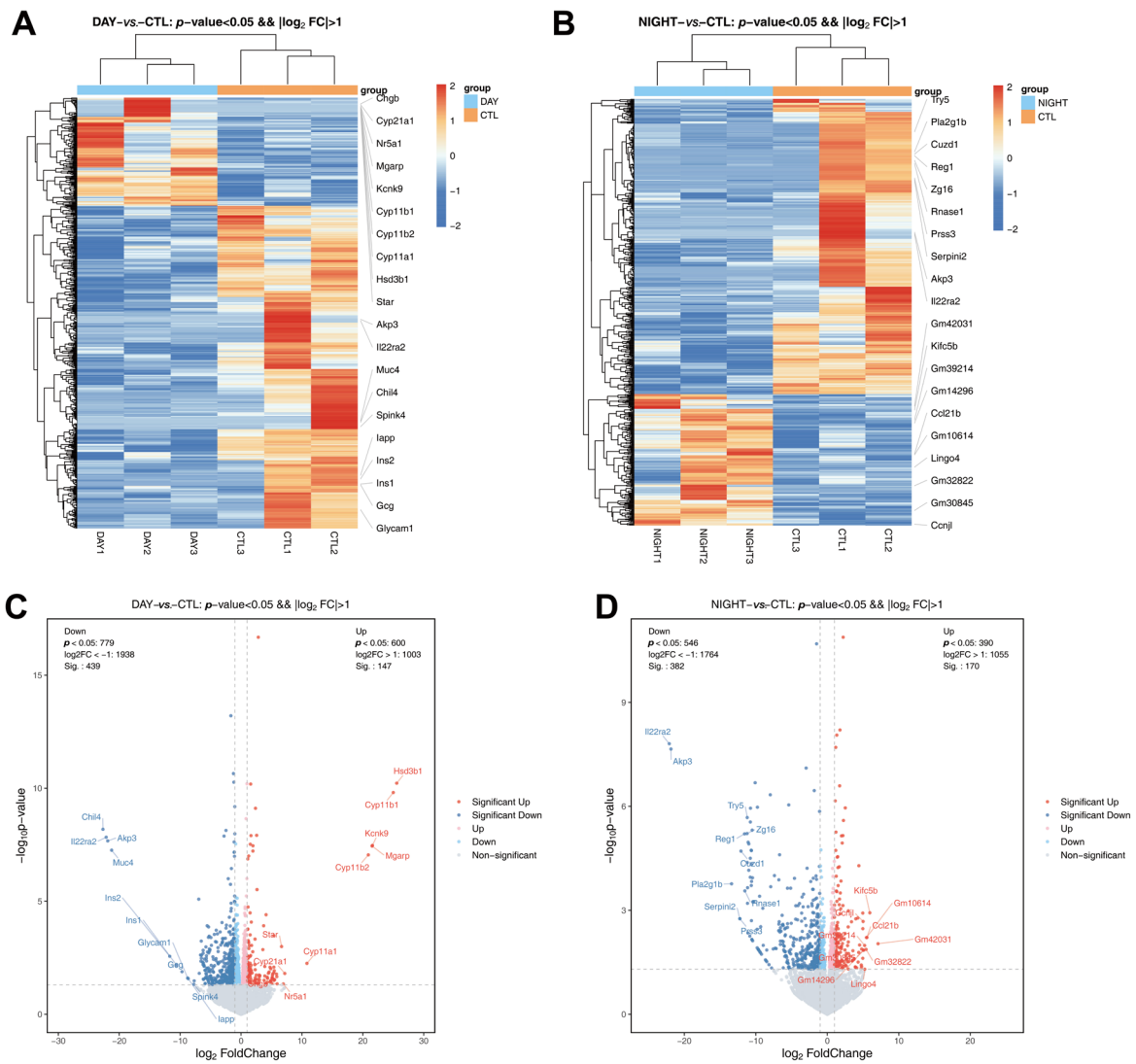

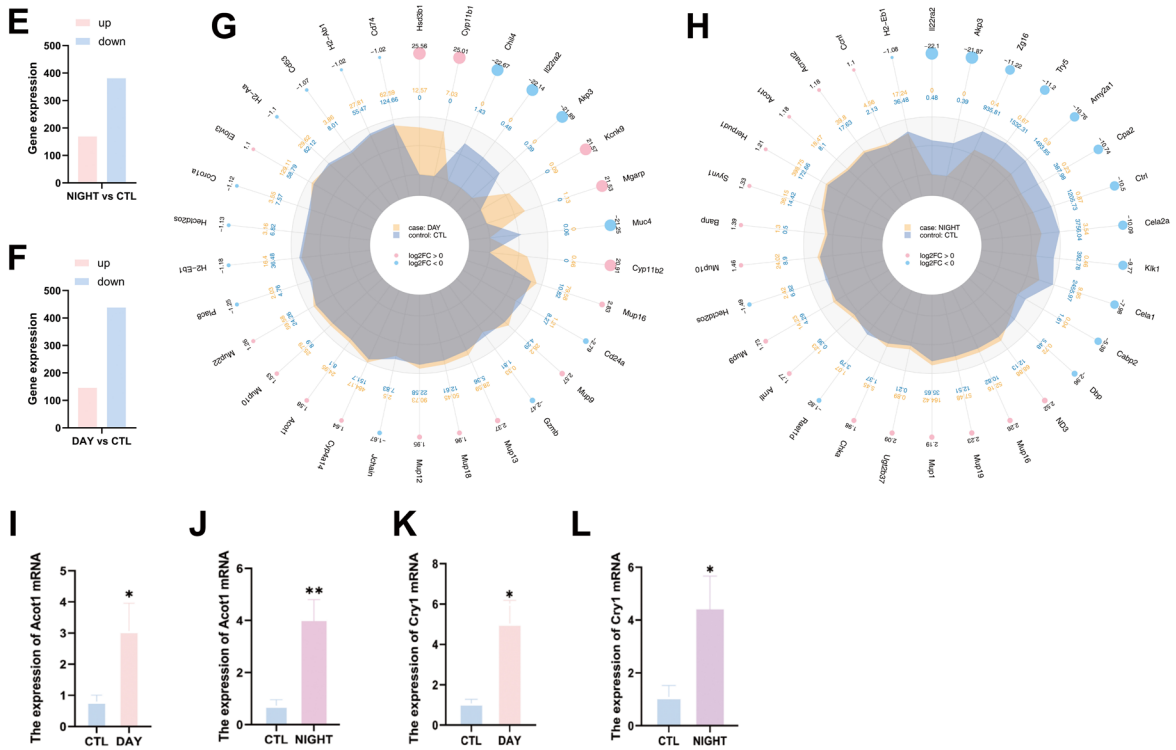

Fig. 1 Cold exposure alters gene expression profiles in the mouse liver

(A) Gene expression heatmap between the control and day groups. (B) Gene expression heatmap between the control and night groups. (C) The volcano plots of differentially expressed genes between the control and day groups. (D) The volcano plots of differentially expressed genes between the control and night groups. (E) The number of DEGs between the control and night groups. (F) The number of DEGs between the control and day groups. (G) Radar Chart of differentially expressed genes between the control and day groups. (H) Radar Chart of differentially expressed genes between the control and night groups. (I) Acot1 mRNA expression in the control and day groups. (J) Acot1 mRNA expression in the control and night groups. (K) Cry1 mRNA expression in the control and day groups. (L) Cry1 mRNA expression between the control and day groups. CTL, control. $^{*}P < 0.05$. $^{**}P < 0.01$.

and $P < 0.05$ (Fig. 1C and D). A total of 586 DEGs were identified between the control and day groups, with 147 upregulated and 439 downregulated (Fig. 2E and Table S1). Similarly, 552 DEGs were identified between the control and night groups, including 170 upregulated and 382 downregulated genes (Fig. 2F and Table S2). A radar chart illustrated gene expression changes relative to the baseline control group (Fig. 1G and H). Additionally, several DEGs were validated using RT-PCR (Fig. 1I-L), with results consistent with RNA sequencing data.

3.2 Enrichment analysis of DEGs

GO, KEGG, and Reactome enrichment analyses were performed using the DEGs. The DEGs between the control and day groups were enriched in GO terms including "membrane (GO: 0016020)", "cytoplasm (GO: 0005737)", and "plasma membrane (GO: 0005886)" (Fig. 2A). The enriched KEGG pathways including "PI3K-Akt signaling pathway", "cytokine-cytokine receptor interaction", and "cell adhesion molecules" (Fig. 2B). Additionally, the enriched Reactome pathways mainly include "immune system" and "signal transduction" (Fig. 2C). Similarly, the DEGs between the control and night groups were enriched in GO terms such as "membrane (GO: 0016020)", "cytoplasm (GO: 0005737)", and "plasma membrane (GO: 0005886) (Fig. 3D). The enriched KEGG pathways included "pancreatic secretion", "neuroactive ligand-receptor interaction", and "protein digestion and absorption" (Fig. 2E). Additionally, the enriched Reactome pathways mainly include "immune system" and "signal transduction" (Fig. 2F). Next, we identified genes that were altered in both the day and night groups. A total of 27 genes (9 upregulated and 18 downregulated) were associated with cold exposure (Fig. 2G). The 9 upregulated genes were associated with "Cushing syndrome", "steroid hormone biosynthesis", and "cortisol synthesis and secretion" (Fig. 2H). The 18 downregulated genes were enriched in "pancreatic secretion", "PI3K-Akt signaling pathway", and "cytokine-cytokine receptor interaction" (Fig. 2I).

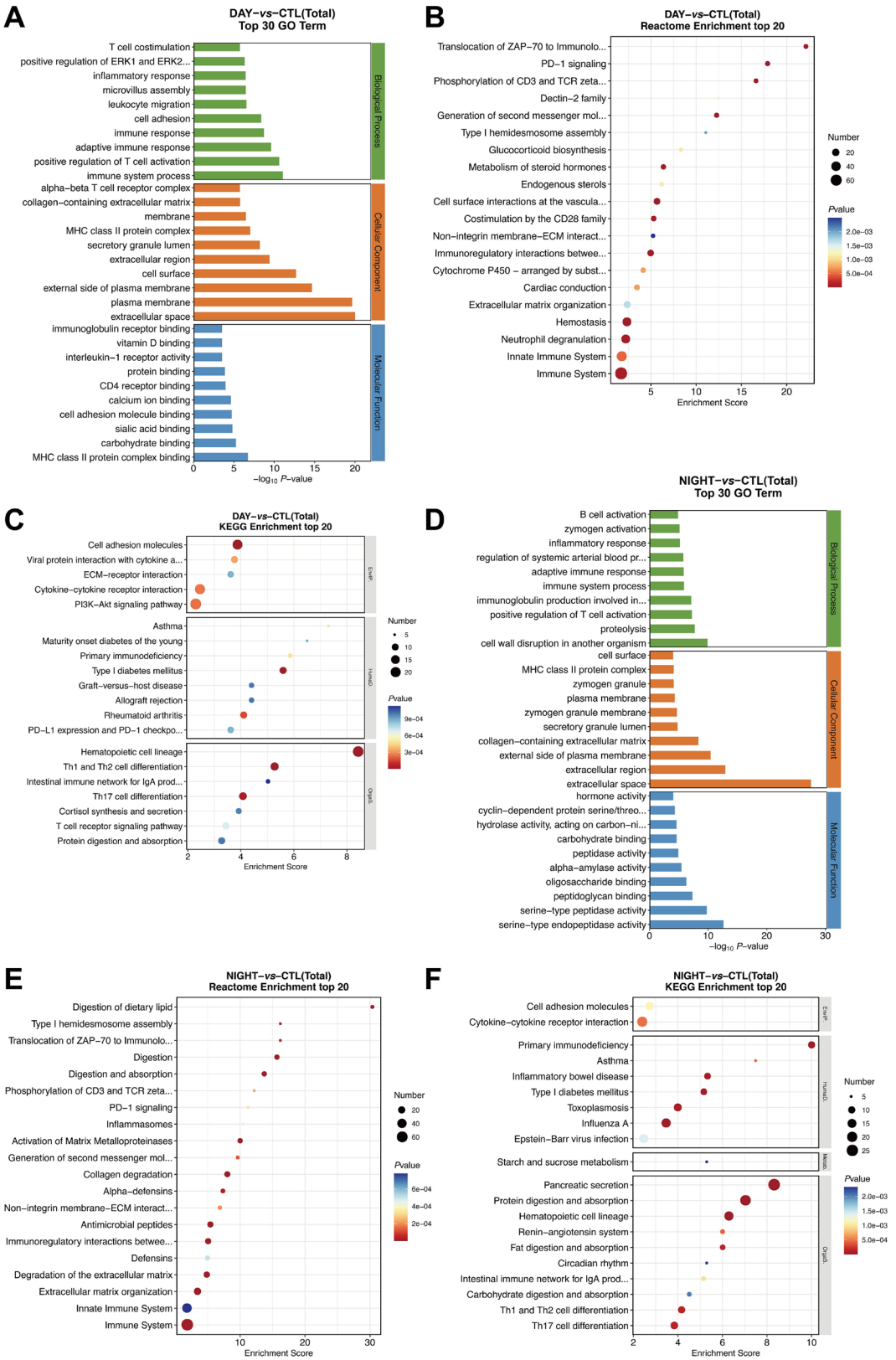
A
DAY−vs−CTL(Total)
Top 30 GO Term
T cell costimulation
positive regulation of ERK1 and ERK2...
inflammatory response
microvillus assembly
leukocyte migration
cell adhesion
immune response
adaptive immune response
positive regulation of T cell activation
immune system process
alpha−beta T cell receptor complex
collagen−containing extracellular matrix
membrane
MHC class II protein complex
secretory granule lumen
extracellular region
cell surface
external side of plasma membrane
plasma membrane
extracellular space
immunoglobulin receptor binding
vitamin D binding
interleukin−1 receptor activity
protein binding
CD4 receptor binding
calcium ion binding
cell adhesion molecule binding
sialic acid binding
carbohydrate binding
MHC class II protein complex binding
Biological Process
Cellular Component
Molecular Function
−log10 P−value
B
DAY−vs−CTL(Total)
Reactome Enrichment top 20
Translocation of ZAP−70 to Immunolo...
PD−1 signaling
Phosphorylation of CD3 and TCR zeta...
Dectin−2 family
Generation of second messenger mol...
Type I hemidesmosome assembly
Glucocorticoid biosynthesis
Metabolism of steroid hormones
Endogenous sterols
Cell surface interactions at the vascula...
Costimulation by the CD28 family
Non−integrin membrane−ECM interact...
Immunoregulatory interactions betwee...
Cytochrome P450 − arranged by subst...
Cardiac conduction
Extracellular matrix organization
Hemostasis
Neutrophil degranulation
Innate Immune System
Immune System
Enrichment Score
Number
Pvalue
C
DAY−vs−CTL(Total)
KEGG Enrichment top 20
Cell adhesion molecules
Viral protein interaction with cytokine a...
ECM−receptor interaction
Cytokine−cytokine receptor interaction
PI3K−Akt signaling pathway
Asthma
Maturity onset diabetes of the young
Primary immunodeficiency
Type I diabetes mellitus
Graft−versus−host disease
Allograft rejection
Rheumatoid arthritis
PD−L1 expression and PD−1 checkpo...
Hematopoietic cell lineage
Th1 and Th2 cell differentiation
Intestinal immune network for IgA prod...
Th17 cell differentiation
Cortisol synthesis and secretion
T cell receptor signaling pathway
Protein digestion and absorption
Enrichment Score
Number
Pvalue
D
NIGHT−vs−CTL(Total)
Top 30 GO Term
B cell activation
zymogen activation
inflammatory response
regulation of systemic arterial blood pr...
adaptive immune response
immune system process
immunoglobulin production involved in...
positive regulation of T cell activation
proteolysis
cell wall disruption in another organism
cell surface
MHC class II protein complex
zymogen granule
plasma membrane
zymogen granule membrane
secretory granule lumen
collagen−containing extracellular matrix
external side of plasma membrane
extracellular region
extracellular space
hormone activity
cyclin−dependent protein serine/threo...
hydrolase activity, acting on carbon−ni...
carbohydrate binding
peptidase activity
alpha−amylase activity
oligosaccharide binding
peptidoglycan binding
serine−type peptidase activity
serine−type endopeptidase activity
Biological Process
Cellular Component
Molecular Function
−log10 P−value
E
NIGHT−vs−CTL(Total)
Reactome Enrichment top 20
Digestion of dietary lipid
Type I hemidesmosome assembly
Translocation of ZAP−70 to Immunolo...
Digestion
Digestion and absorption
Phosphorylation of CD3 and TCR zeta...
PD−1 signaling
Inflammasomes
Activation of Matrix Metalloproteinases
Generation of second messenger mol...
Collagen degradation
Alpha−defensins
Non−integrin membrane−ECM interact...
Antimicrobial peptides
Immunoregulatory interactions betwee...
Defensins
Degradation of the extracellular matrix
Extracellular matrix organization
Innate Immune System
Immune System
Enrichment Score
Number
Pvalue
F
NIGHT−vs−CTL(Total)
KEGG Enrichment top 20
Cell adhesion molecules
Cytokine−cytokine receptor interaction
Primary immunodeficiency
Asthma
Inflammatory bowel disease
Type I diabetes mellitus
Toxoplasmosis
Influenza A
Epstein−Barr virus infection
Starch and sucrose metabolism
Pancreatic secretion
Protein digestion and absorption
Hematopoietic cell lineage
Renin−angiotensin system
Fat digestion and absorption
Circadian rhythm
Intestinal immune network for IgA prod...
Carbohydrate digestion and absorption
Th1 and Th2 cell differentiation
Th17 cell differentiation
Enrichment Score
Number
Pvalue

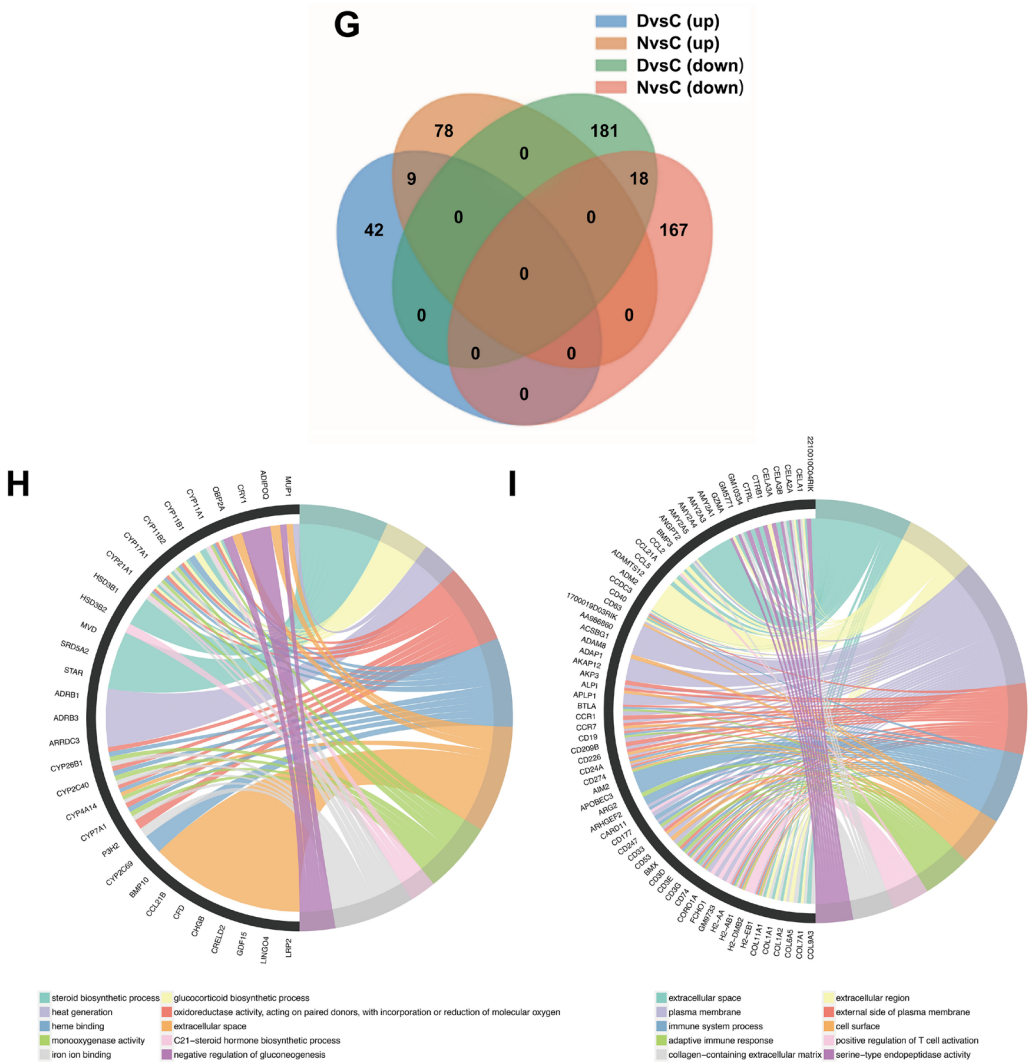

Fig. 2 Enrichment analysis of differentially expressed genes (DEGs) in the mouse liver

(A) The bar chart of gene ontology enrichment analysis of DEGs between the control and day groups. (B) Kyoto encyclopedia of genes and genomes (KEGG) enrichment analysis of DEGs between the control and day groups. (C) Reactome enrichment analysis of DEGs between the control and day groups. (D) GO enrichment analysis of DEGs between the control and night groups. (E) KEGG enrichment analysis of DEGs between the control and night groups. (F) Reactome enrichment analysis of DEGs between the control and night groups. (G) The overlapped DEGs across the three groups. (H) KEGG pathway of DEGs is upregulated following cold exposure. (I) KEGG pathway of DEGs is downregulated following cold exposure. CTL, control.

3.3 DEMs in the mouse liver tissue following cold exposure

Metabolites in liver tissues were detected using liquid chromatography-mass spectrometry (LC-MS). The Base Peak Chromatogram revealed metabolic differences among the groups in both positive and negative ion models (Fig. S1). OPLS-DA was conducted to identify variations in metabolites among the three groups (Fig. 3A and B). The model's prediction results confirmed the reliability of the OPLS-DA analysis (Fig. 3C and D). The heatmap illustrated metabolite expression differences in each group (Fig. 3E and F). A total of 239 metabolites were differentially expressed between the control and day groups, with 123 upregulated and 116 downregulated (Fig. 3G and Table S3). The most significant altered DEMs between the control and day groups are shown in the lollipop chart (Fig. 5I). Similarly, 241 metabolites were differentially expressed between the control group and the night group, with 128 upregulated and 113 downregulated (Fig. 3H and Table S4). The most significant altered DEMs between the control and night groups are shown in the lollipop chart (Fig. 3J). Some DEMs overlapped between the day and night groups (Fig. 3K).

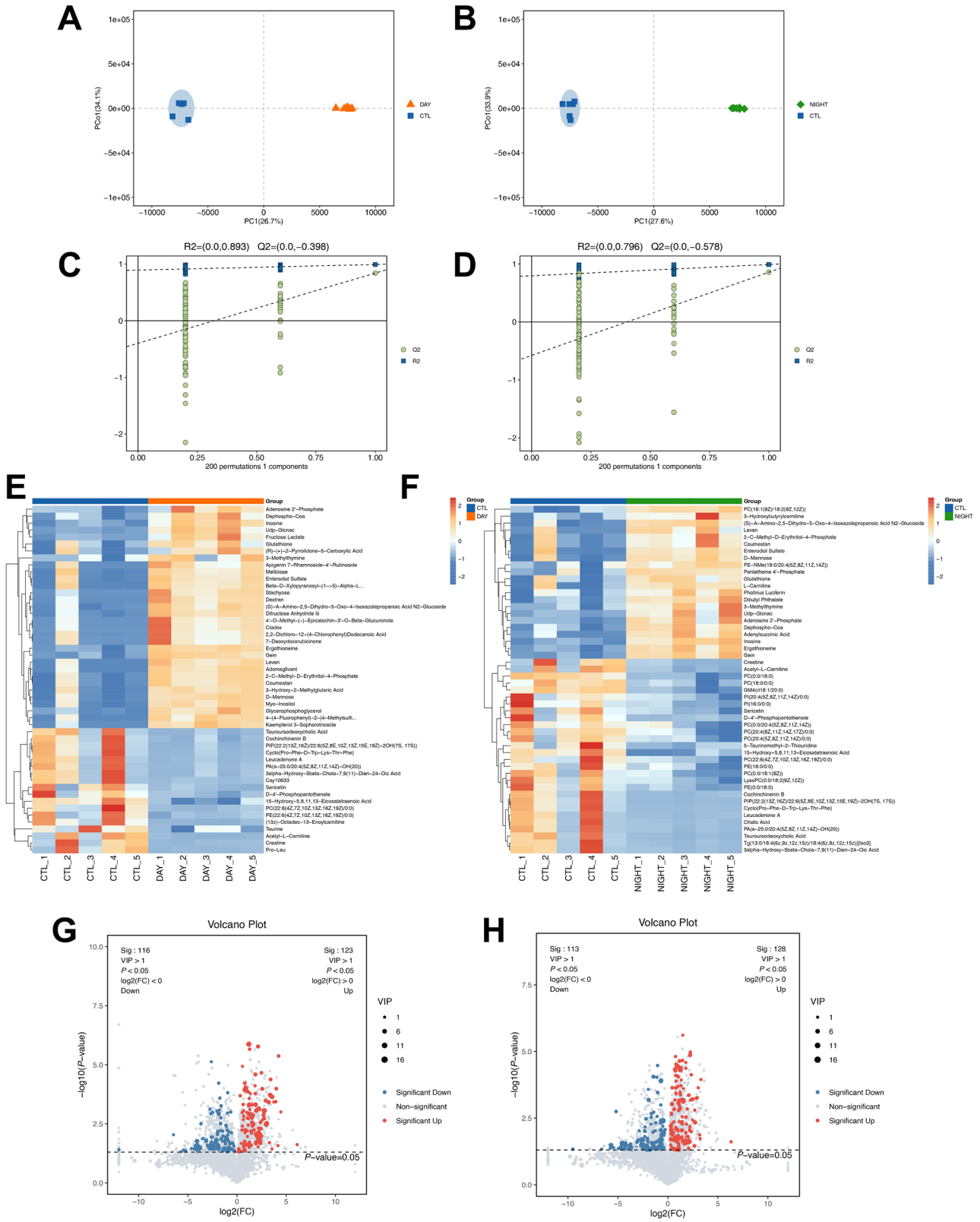
A
PCo1(34.1%)
PC1(26.7%)
DAY
CTL
B
PCo1(33.9%)
PC1(27.6%)
NIGHT
CTL
C
R2=(0.0,0.893) Q2=(0.0,−0.398)
200 permutations 1 components
Q2
R2
D
R2=(0.0,0.796) Q2=(0.0,−0.578)
200 permutations 1 components
Q2
R2
E
Group
CTL
DAY
CTL_1 CTL_2 CTL_3 CTL_4 CTL_5 DAY_1 DAY_2 DAY_3 DAY_4 DAY_5
F
Group
CTL
NIGHT
CTL_1 CTL_2 CTL_3 CTL_4 CTL_5 NIGHT_1 NIGHT_2 NIGHT_3 NIGHT_4 NIGHT_5
G
Volcano Plot
Sig : 116
VIP > 1
P < 0.05
log2(FC) < 0
Down
Sig : 123
VIP > 1
P < 0.05
log2(FC) > 0
Up
VIP
1
6
11
16
Significant Down
Non−significant
Significant Up
−log10(P−value)
P−value=0.05
log2(FC)
H
Volcano Plot
Sig : 113
VIP > 1
P < 0.05
log2(FC) < 0
Down
Sig : 128
VIP > 1
P < 0.05
log2(FC) > 0
Up
VIP
1
6
11
16
Significant Down
Non−significant
Significant Up
−log10(P−value)
P−value=0.05
log2(FC)

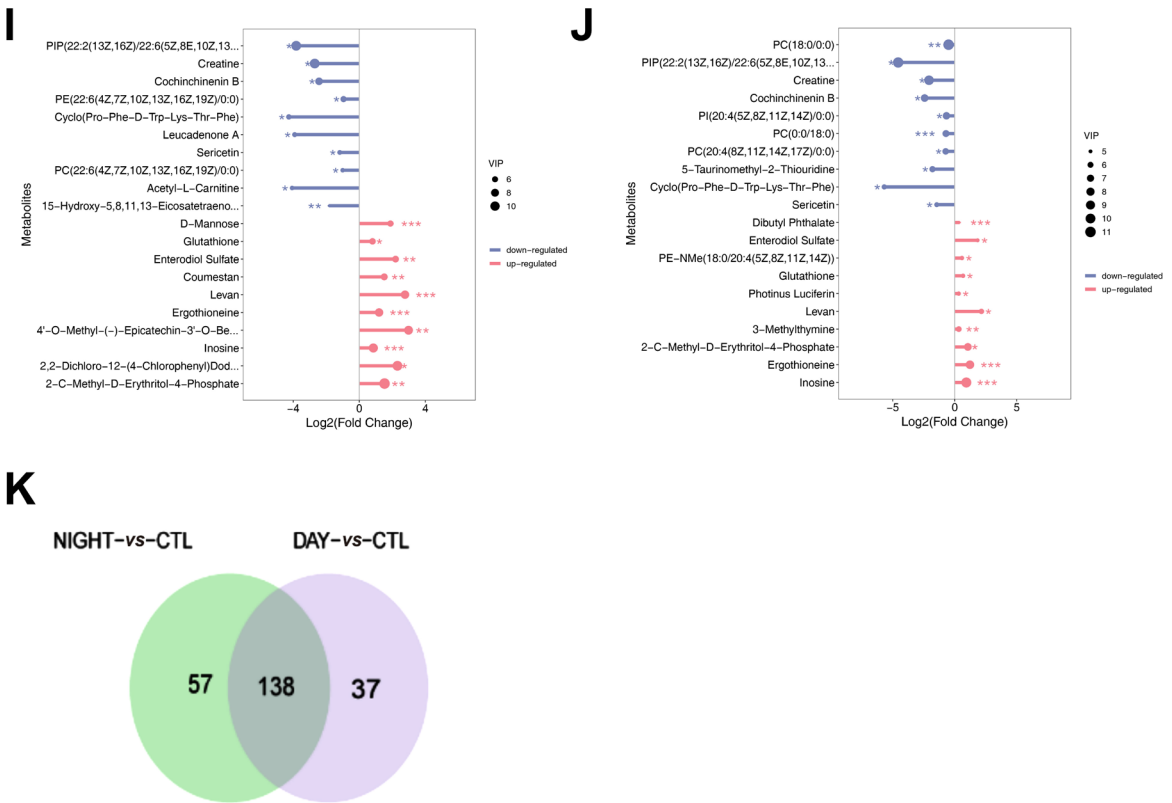

Fig. 3 Enrichment analysis of differentially expressed metabolites (DEMs) in the mouse liver tissue

(A) Orthogonal partial least squares discriminant analysis (OPLS-DA) analysis of the cardiometabolic group between the control and day positive ion (POS) mode. (B) OPLS-DA of the cardiometabolic group between the control and night in POS mode. (C) Permutation test evaluating the accuracy of the OPLS-DA model for the control and day group. (D) Permutation test evaluating the accuracy of the OPLS-DA model for the control and night group. (E) Heatmap of DEMs between the control and day groups. (F) Heatmap of DEMs between the control and night groups. (G) Volcano plots of DEMs between the control and day groups. (H) Volcano plots of DEMs between the control and night groups. (I) Lollipop chart of DEMs between the control and day groups. (J) Lollipop chart of DEMs between the control and night groups. (K) Venn diagram of DEMs across the three groups. CTL, control.

3.4 Enrichment analysis of DEMs

KEGG pathway analysis was performed using the DEMs. The results showed that the DEMs between the control and day groups were enriched in KEGG pathways, including "membrane transport", "nucleotide metabolism", and "metabolism of cofactors and vitamins" (Fig. 4A). The upregulated DEMs were primarily enriched in "ABC transporters" and "purine metabolism", while the downregulated DEMs were enriched in "protein digestion and absorption" and "aminoacyl-tRNA biosynthesis" (Fig. 4B). Mapping the DEMs to the Reactome database revealed enrichment in pathways such as "transport of small molecules", "SLC-mediated transmembrane transport", and "metabolism of nucleotides" (Fig. 4C). For the DEMs between the control and night groups, enriched KEGG pathways included "ABC transporters", "purine metabolism", and "ferroptosis" (Fig. 4D). The upregulated DEGs were enriched in "pyrimidine metabolism" and "purine metabolism", whereas the downregulated DEMs were enriched in "ABC transporters" and "ferroptosis" (Fig. 4E). Similarly, mapping these DEMs to the Reactome database highlighted enrichment in pathways related to "transport of small molecules", "SLC-mediated transmembrane transport", and "metabolism of nucleotides" (Fig. 4F). Additionally, enriched pathways were identified using GSEA (Fig. 4G and H).

3.5 Integration of transcriptomic and metabolomic data

We integrated the KEGG enrichment analysis results from both the transcriptomic and metabolomic data. In the comparison between the control and day groups, DEGs were enriched in 136 pathways, while DEMs were enriched in 98 pathways (Fig. 5A). A total of 37 overlapping pathways were identified, including "alanine, aspartate and glutamate metabolism" and

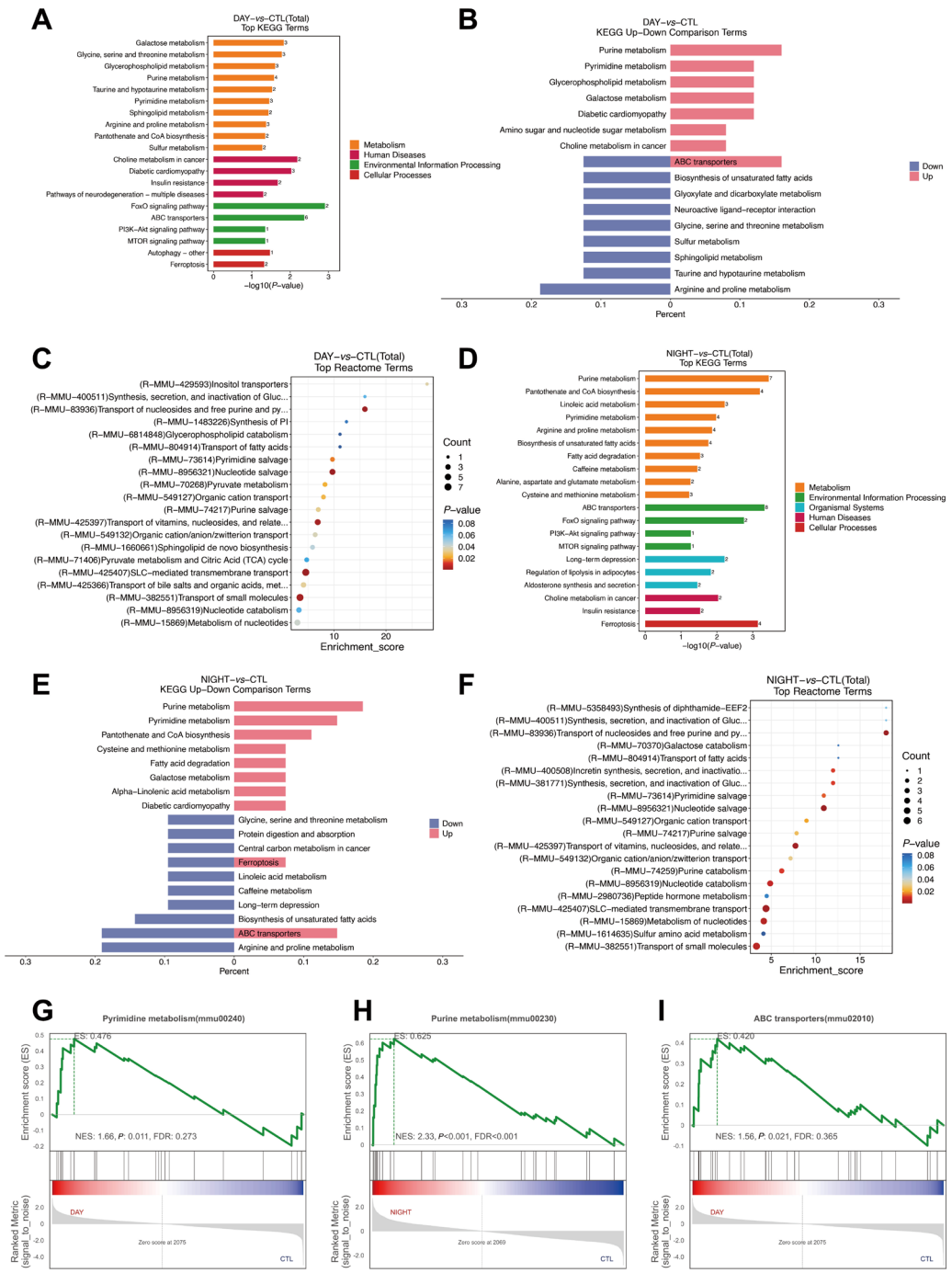

Fig. 4 Enrichment analysis of the differentially expressed metabolites (DEMs) in liver of cold-exposed mice

(A) KEGG enrichment analysis of DEMs between the control and day groups. (B) Kyoto encyclopedia of genes and genomes (KEGG) enrichment analysis of the upregulated and downregulated DEMs between the control and day groups. (C) Reactome enrichment analysis of DEMs between the control and day groups. (D) KEGG enrichment analysis of DEMs between the control and night groups. (E) KEGG enrichment analysis of the upregulated and downregulated DEMs between the control and night groups. (F) Reactome enrichment analysis of DEMs between the control and night groups. (G) Gene set enrichment analysis (GSEA) enrichment analysis of Purine metabolism pathway between the control and day groups. (H) GSEA enrichment analysis of Purine metabolism pathway between the control and night groups. (I) GSEA enrichment analysis of ABC transporters pathway between the control and day groups. CTL, control.

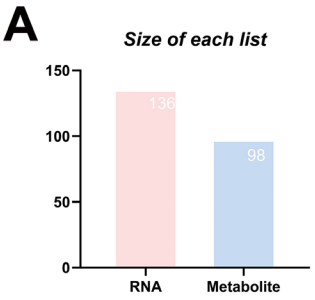
A
Size of each list
150
100
50
0
136
98
RNA
Metabolite

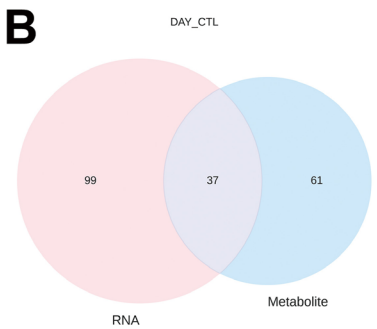
B
DAY_CTL
99
37
61
RNA
Metabolite

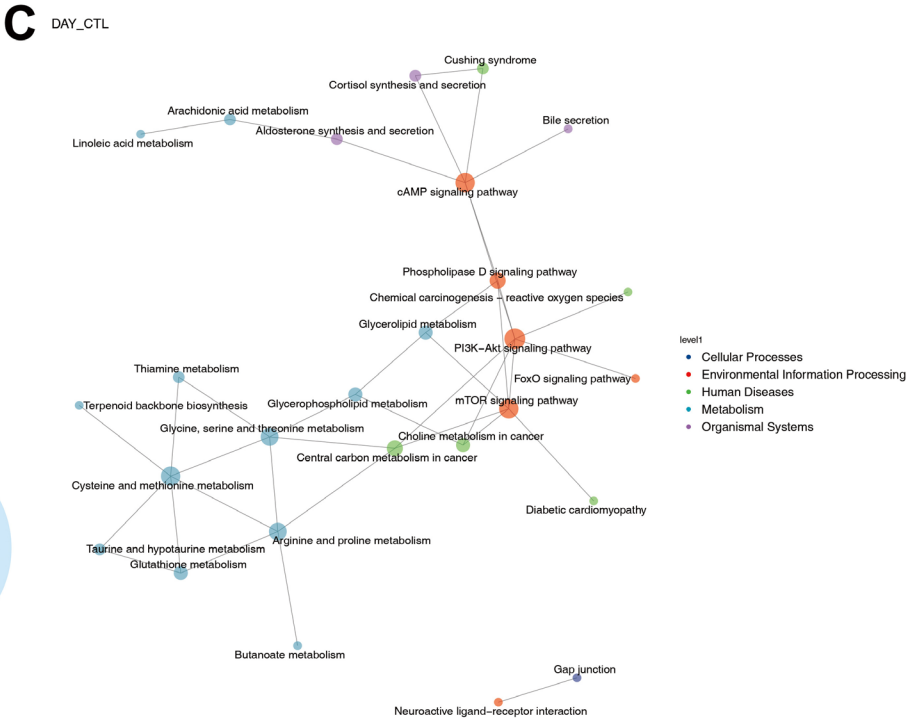
C
DAY_CTL
Cushing syndrome
Cortisol synthesis and secretion
Arachidonic acid metabolism
Aldosterone synthesis and secretion
Bile secretion
Linoleic acid metabolism
cAMP signaling pathway
Phospholipase D signaling pathway
Chemical carcinogenesis - reactive oxygen species
Glycerolipid metabolism
PI3K-Akt signaling pathway
Thiamine metabolism
FoxO signaling pathway
Terpenoid backbone biosynthesis
Glycerophospholipid metabolism
mTOR signaling pathway
Glycine, serine and threonine metabolism
Choline metabolism in cancer
Central carbon metabolism in cancer
Cysteine and methionine metabolism
Diabetic cardiomyopathy
Arginine and proline metabolism
Taurine and hypotaurine metabolism
Glutathione metabolism
Butanoate metabolism
Gap junction
Neuroactive ligand-receptor interaction
level1
Cellular Processes
Environmental Information Processing
Human Diseases
Metabolism
Organismal Systems

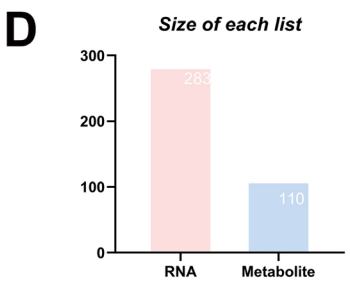
D
Size of each list
300
200
100
0
283
110
RNA
Metabolite

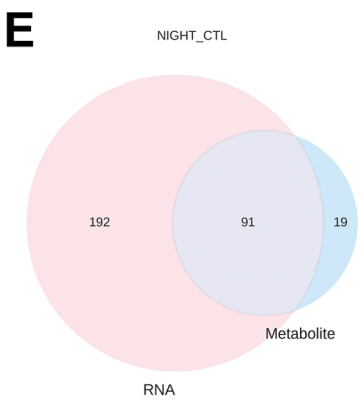
E
NIGHT_CTL
192
91
19
Metabolite
RNA

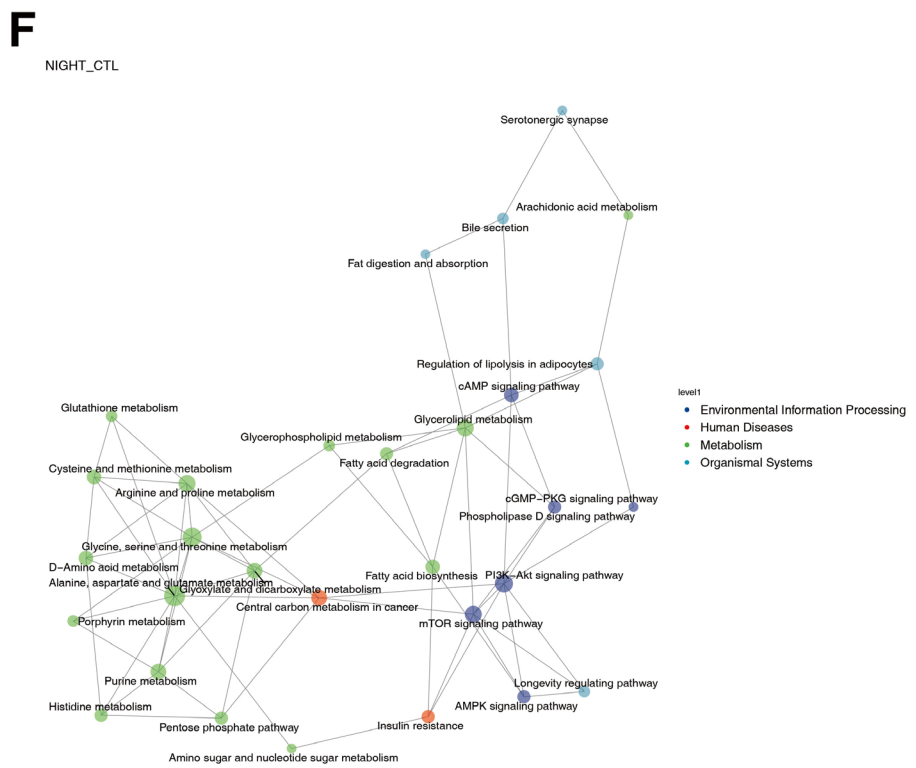
F
NIGHT_CTL
Serotonergic synapse
Arachidonic acid metabolism
Bile secretion
Fat digestion and absorption
Regulation of lipolysis in adipocytes
cAMP signaling pathway
Glutathione metabolism
Glycerolipid metabolism
Glycerophospholipid metabolism
Fatty acid degradation
Cysteine and methionine metabolism
Arginine and proline metabolism
cGMP-PKG signaling pathway
Phospholipase D signaling pathway
Glycine, serine and threonine metabolism
D-Amino acid metabolism
Fatty acid biosynthesis
PI3K-Akt signaling pathway
Alanine, aspartate and glutamate metabolism
Glyoxylate and dicarboxylate metabolism
Central carbon metabolism in cancer
Porphyrin metabolism
mTOR signaling pathway
Purine metabolism
Longevity regulating pathway
Histidine metabolism
AMPK signaling pathway
Pentose phosphate pathway
Insulin resistance
Amino sugar and nucleotide sugar metabolism
level1
Environmental Information Processing
Human Diseases
Metabolism
Organismal Systems

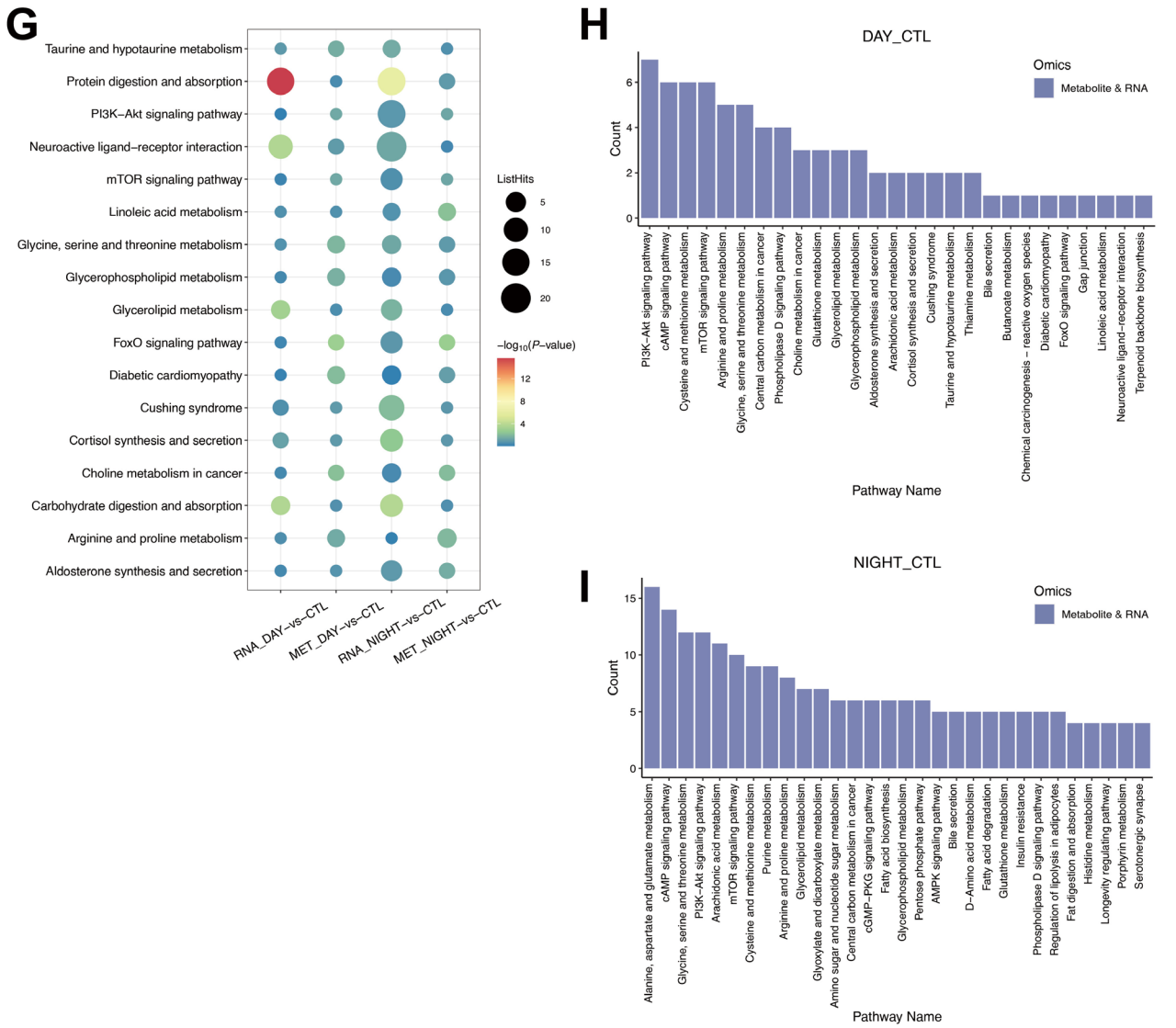

Fig. 5 Combined analysis of transcriptome and metabolome

(A) Number of differentially expressed metabolites (DEMs) and differentially expressed metabolites (DEMs) between the control and day groups enriched Kyoto encyclopedia of genes and genomes (KEGG) pathways. (B) Number of overlapped KEGG pathways between the control and day groups. (C) Overlapping pathways between the control and day groups. (D) Number of DEGs and DEMs between the control and night groups enriched KEGG pathways. (E) Number of overlapping KEGG pathways between the control and night groups. (F) Overlapping pathways between the control and night groups. (G) Interaction network diagram of the overlapping pathways between the control and day groups. (H) Interaction network diagram of overlapping pathways between the control and night groups. (I) Enriched pathways associated with cold exposure. CTL, control.

"cAMP signaling pathway" (Fig. 5B and C). The correlation of overlapping pathways was illustrated in the pathway network (Fig. 5G). For the comparison between the control and night groups, DEGs were enriched in 283 pathways, while DEMs were enriched in 110 pathways (Fig. 5D). A total of 91 overlapping pathways were identified, including "alanine, aspartate and glutamate metabolism" and "cAMP signaling pathway" (Fig. 5E and F). The correlation of these overlapping pathways was also illustrated in the pathway network (Fig. 5G). Additionally, some pathways were specifically associated with cold exposure, including the "cAMP signaling pathway" and the "PI3K-Akt signaling pathway" (Fig. 5H and I).

4 Discussion

Cold exposure has the potential to modify the metabolic state of organisms. Huang *et al.* demonstrated that cold exposure could induce liver damage by triggering ferroptosis through the p38 MAPK/Drp1 pathway[18]. Conversely, Sugimoto *et al.* found that cold exposure could decrease liver inflammation and improve metabolic disturbances[19]. Several studies have shown that prolonged cold exposure, ranging from weeks to months, results in consistent metabolic alterations, which typically become apparent within a month[20-22]. In the present study, we obtained transcriptome and metabolome data from the liver of cold-exposed mice. We then conducted a comprehensive analysis and identified key pathways associated with cold exposure.

RNA sequencing results showed that cold exposure altered gene expression profiles in the liver of mice. A total of 586 and 552 DEGs were identified in the day and night groups, respectively. Some of these genes are closely related to liver lipid metabolism, such as *Cyp11a1*, *Cyp11b1*, and *Cyp11b2*. Perepechaeva *et al.* found that cold activates cytochromes P450 subfamilies, which play an important role in cholesterol degradation[23]. Subsequently, enrichment analysis was performed using the DEGs. In the day group, DEGs were enriched in KEGG pathways, such as the "PI3K-Akt signaling pathway", "cytokine-cytokine receptor interaction", and "cell adhesion molecules". In the night group, DEGs were enriched in pathways including "pancreatic secretion", "neuroactive ligand-receptor interaction", and "protein digestion and absorption". Some pathways overlapped between the day and night groups, including the "PI3K-Akt signaling pathway", "cytokine-cytokine receptor interaction", indicating that these pathways were not affected by time periods within a 24-hour cycle. Wang *et al.* revealed that cold exposure could activate the Akt pathway, consequently enhancing hepatic ATP production[24]. Yin *et al.* found that cytokine-cytokine receptor interaction is closely related to high-fat diet-induced non-alcoholic fatty liver disease[25]. Non-targeted metabolomics analysis results showed significant differences in metabolites among the three groups. A total of 239 and 241 DEMs were identified in the day and night groups, respectively. Cold exposure altered the expression levels of several bioactive metabolites. For instance, ergothioneine levels were upregulated under cold stress, suggesting a potential role reducing oxidative stress and inflammation[26]. Glutathione levels were also elevated in the cold-exposed group, which is crucial for antioxidation, detoxification, cell membrane protection, amino acid metabolism, and immune regulation in the liver[27]. These findings suggest that cold exposure induces metabolic reprograming.

Enrichment analysis of the DEMs revealed that the DEMs in the control *vs.* day group were enriched in pathways such as "ABC transporters", "purine metabolism", and "Bile secretion". Meanwhile, the DEMs in the control *vs.* night groups were enriched in "ABC transporters" and "ferroptosis". The "ABC transporters" pathway was common to both day and night groups. This pathway is involved in the excretion of drugs, toxins, and metabolites, thereby protecting the liver from toxic substances[28]. Wang *et al.* suggested that targeting ABC transporters and modulating bile acid toxicity could be a potential intervention strategy to alleviate chronic inflammation and reduce the incidence of liver cancer[29]. Additionally, we found that compared with the day group, the ferroptosis pathway was significantly enriched in the night group. Several studies have also reported that cold exposure promotes ferroptosis, leading to liver injury[18,30]. These findings suggest that changes of clock genes may contribute to liver damage, warranting further investigation. To further elucidate the mechanisms underlying cold exposure-induced liver changes, we integrated transcriptome and metabolome data. Combined analysis suggested that several pathways, including the "cAMP signaling pathway" and the "PI3K-Akt signaling pathway," may be involved in cold exposure responses. Jiao *et al.* found that the cAMP pathway plays a role in the liver injury during long-term supercooled liver preservation[31]. Additionally, the cAMP response element-binding protein (CREB) facilitates the oxidative breakdown of fatty acids in hepatocytes, playing a crucial role in fatty acid oxidation in MAFLD[32]. Several studies have demonstrated that the PI3K-Akt pathway protects the liver through multiple mechanisms, including promoting cell survival, antioxidation, anti-inflammation, and metabolic regulation[33-35]. Wu *et al.* found that quercetin attenuates bile duct ligation (BDL)- or carbon tetrachloride (CCl4)-induced liver injury by activating the PI3K/Akt signaling pathway[36]. Based on these findings, we speculate that these pathways may be involved in metabolic changes in the mouse liver under cold exposure.

Although our integrated analysis revealed altered pathways, the study is primarily descriptive, and the lack of functional validation limits our ability to conclusively determine the key drivers of the metabolic response to cold exposure.

5 Conclusion

Cold exposure altered liver transcriptomic and metabolomic profiles in mice. The integrative analysis of transcriptomic and metabolomic data highlights the complexity of the physiological response to cold exposure. These findings provide new insights for future research on cold adaptation and shed light on the interplay between gene expression and metabolic profiles in

response to environmental challenges.

Acknowledgement

Not applicable.

Research ethics

All experimental procedures were conducted in full compliance with the Guide for the Care and Use of Laboratory Animals. The study was pre-approved by the Ethics Committee of College of Pharmacy, Harbin Medical University (No. IRB3057723).

Informed consent

Not applicable.

Author contributions

Jiang Y N, Qu B, and Wang S contributed to the conception and design of the study. Di Y Z, Wen Z C, and Zhang K J wrote or contributed to the writing of the manuscript. Shen X Y, Shi C P, and Liu X M performed the biological experiments. Di Y Z, Wen Z C, Chao Y Q, and Wang X conducted the bioinformatics analysis. All authors reviewed and approved the final manuscript.

Use of Large Language Models, AI and Machine Learning Tools

No large language models, AI or machine learning tool was used for any part of the present study.

Conflicts of interest

The authors declare no competing financial interests.

Research funding

This work was supported by the National Natural Science Foundation of China (82370269), the Heilongjiang Postdoctoral Foundation (LBH-Q21134 and LBH-Z22226), and Harbin Medical University Science Foundation (2023).

Data availability

The data that support the findings of this study are available from the corresponding author upon reasonable request.

References

[1] Thorne R H, Purcell A T. Environmental effects on the subjective perception of level of arousal and the human body temperature rhythm. Int J Biometeorol, 1976; 20(4): 318-324.
[2] Barnett A G, Sans S, Salomaa V, *et al.* The effect of temperature on systolic blood pressure. Blood Press Monit, 2007; 12(3): 195-203.
[3] Liu S, Liu Y, Wan B, *et al.* Association between vitamin D status and non-alcoholic fatty liver disease: A population-based study. J Nutr Sci Vitaminol (Tokyo), 2019; 65(4): 303-308.
[4] Yip T C, Fan J G, Wong V W. China's fatty liver crisis: A looming public health emergency. Gastroenterology, 2023; 165(4): 825-827.
[5] Liu Y, Xue N, Zhang B, *et al.* Cold stress induced liver injury of mice through activated NLRP3/Caspase-1/GSDMD pyroptosis signaling pathway. Biomolecules, 2022; 12(7): 927.
[6] Ivanova Y M, Blondin D P. Examining the benefits of cold exposure as a therapeutic strategy for obesity and type 2 diabetes. J Appl Physiol (1985), 2021; 130(5): 1448-1459.
[7] Costello J T, Baker P R, Minett G M, *et al.* Whole-body cryotherapy (extreme cold air exposure) for preventing and treating muscle soreness after exercise in adults. Cochrane Database Syst Rev, 2015; 2015(9): CD010789.
[8] Cunningham J J, Gulino M A, Meara P A, *et al.* Enhanced hepatic insulin sensitivity and peripheral glucose uptake in cold acclimating rats. Endocrinology, 1985; 117(4): 1585-1589.
[9] Peschke D, Peschke E, Peil J, *et al.* Effect of ganglionectomy (superior cervical ganglia) at normal temperature and exposure to cold on the circadian rhythm of liver glycogen and blood glucose levels of the Wistar rat with regard to the pineal gland. Acta Histochem, 1986; 80(2): 159-174.
[10] Xu J, Cui L, Wang J, *et al.* Cold-activated brown fat-derived extracellular vesicle-miR-378a-3p stimulates hepatic gluconeogenesis in male mice. Nat Commun, 2023; 14(1): 5480.
[11] Gong L, Zhao S, Chu X, *et al.* Assessment of cold exposure-induced metabolic changes in mice using untargeted metabolomics. Front Mol Biosci, 2023; 10:1228771.
[12] Yu X X, Mao W, Zhong A, *et al.* Characterization of novel UCP5/BMCP1 isoforms and differential regulation of UCP4 and UCP5 expression through dietary or temperature manipulation. FASEB J, 2000; 14(11): 1611-1618.
[13] Kim D, Langmead B, Salzberg S L. HISAT: a fast spliced aligner with low memory requirements. Nat Methods, 2015; 12(4): 357-360.
[14] Huang X, Tang W, Lin C, *et al.* Protective mechanism of Astragalus Polysaccharides against Cantharidin-induced liver injury determined *in vivo* by liquid chromatography/mass spectrometry metabolomics. Basic Clin Pharmacol Toxicol, 2021; 129(1): 61-71.
[15] Ashburner M, Ball C A, Blake J A, *et al.* Gene ontology: tool for the unification of biology. The Gene Ontology Consortium. Nat Genet, 2000; 25(1): 25-29.
[16] Kanehisa M, Araki M, Goto S, *et al.* KEGG for linking genomes to

life and the environment. Nucleic Acids Res, 2008; 36(Database issue): D480-D484.
[17] Subramanian A, Tamayo P, Mootha V K, *et al.* Gene set enrichment analysis: a knowledge-based approach for interpreting genome-wide expression profiles. Proc Natl Acad Sci U S A, 2005; 102(43): 15545-15550.
[18] Huang Y, Xiong K, Wang A, *et al.* Cold stress causes liver damage by inducing ferroptosis through the p38 MAPK/Drp1 pathway. Cryobiology, 2023; 113: 104563.
[19] Sugimoto S, Mena H A, Sansbury B E, *et al.* Brown adipose tissue-derived MaR2 contributes to cold-induced resolution of inflammation. Nat Metab, 2022; 4(6): 775-790.
[20] Du J, He Z, Cui J, *et al.* Osteocyte apoptosis contributes to cold exposure-induced bone loss. Front Bioeng Biotechnol, 2021; 9: 733582.
[21] Fischer A W, Cannon B, Nedergaard J. Optimal housing temperatures for mice to mimic the thermal environment of humans: An experimental study. Mol Metab, 2018; 7: 161-170.
[22] Lelis Carvalho A, Treyball A, Brooks D J, *et al.* TRPM8 modulates temperature regulation in a sex-dependent manner without affecting cold-induced bone loss. PLoS One, 2021; 16(6): e0231060.
[23] Perepechaeva M L, Grishanova A Y. Cold-induced activities of cytochromes P450 1A1 and 1A2 in rat liver: putative role of endogenous compounds in induction mechanism. Bull Exp Biol Med, 2013; 154(5): 638-641.
[24] Wang J, Chen Y, Zhang W, *et al.* Akt activation protects liver cells from apoptosis in rats during acute cold exposure. Int J Biol Sci, 2013; 9(5): 509-517.
[25] Yin I X, Tang H, Fang Y, *et al.* Hepatic transcriptome delineates the therapeutic effects of Sanren Tang on high-fat diet-induced non-alcoholic fatty liver disease. J Tradit Chin Med, 2023; 43(6): 1092-1102.
[26] Dare A, Channa M L, Nadar A. L-ergothioneine and metformin alleviates liver injury in experimental type-2 diabetic rats *via* reduction of oxidative stress, inflammation, and hypertriglyceridemia. Can J Physiol Pharmacol, 2021; 99(11): 1137-1147.
[27] DeLeve L D, Kaplowitz N. Glutathione metabolism and its role in hepatotoxicity. Pharmacol Ther, 1991; 52(3): 287-305.
[28] Prescher M, Kroll T, Schmitt L. ABCB4/MDR3 in health and disease - at the crossroads of biochemistry and medicine. Biol Chem, 2019; 400(10): 1245-1259.
[29] Wang R, Sheps J A, Ling V. ABC transporters, bile acids, and inflammatory stress in liver cancer. Curr Pharm Biotechnol, 2011; 12(4): 636-646.
[30] Kojima H, Hirao H, Kadono K, *et al.* Cold stress-induced ferroptosis in liver sinusoidal endothelial cells determines liver transplant injury and outcomes. JCI Insight, 2024; 9(3) : e174354.
[31] Jiao X, Li Y, Chen Z, *et al.* Targeting the PDE3B-cAMP-autophagy axis prevents liver injury in long-term supercooling liver preservation. Sci Transl Med, 2024; 16(775): eadk0636.
[32] Zhang J I, Wang S H, Zhao Y J, *et al.* The role and mechanism of CREBH regulating SIRT3 in metabolic associated fatty liver disease. Life Sci, 2022; 306: 120838.
[33] Wang M, Zhang J, Gong N. Role of the PI3K/Akt signaling pathway in liver ischemia reperfusion injury: A narrative review. Ann Palliat Med, 2022; 11(2): 806-817.
[34] Yao Y, Wang L, Jin P, *et al.* Methane alleviates carbon tetrachloride induced liver injury in mice: Anti-inflammatory action demonstrated by increased PI3K/Akt/GSK-3beta-mediated IL-10 expression. J Mol Histol, 2017; 48(4): 301-310.
[35] Zhou Y D, Hou J G, Liu W, *et al.* 20(R)-ginsenoside Rg3, a rare saponin from red ginseng, ameliorates acetaminophen-induced hepatotoxicity by suppressing PI3K/AKT pathway-mediated inflammation and apoptosis. Int Immunopharmacol, 2018; 59: 21-30.
[36] Wu L, Zhang Q, Mo W, *et al.* Quercetin prevents hepatic fibrosis by inhibiting hepatic stellate cell activation and reducing autophagy *via* the TGF-beta1/Smads and PI3K/Akt pathways. Sci Rep, 2017; 7(1): 9289.